A Model-Based Fuzzy Logic Controller With Kalman Filtering for Tracking Mean Arterial Pressure

Shing-Hong Liu and Chin-Teng Lin, *Senior Member, IEEE*

***Abstract*—This paper proposes a new noninvasive measurement method for tracking the tendency of mean arterial pressure (MAP) in the radial artery. The designed system consists of a tonometer, a microsyringe device, and a model-based fuzzy logic controller. The modified flexible diaphragm tonometer is to detect the continuous blood pressure waveform and vessel volume pulse. A precise mathematical model describing the interaction between the tonometer and artery is derived. To reach accurate measurement without distortion, a model-based fuzzy logic control system is designed to compensate the change of MAP by applying a counter pressure on the tonometer chamber through the microsyringe device. The proposed control system consists of a linear predictor, a Kalman filter, and a synthetic fuzzy logic controller (SFLC). The linear predictor is to estimate the MAPs changing tendency based on the identified arterial pressure–volume model and then to beat-to-beat adjust the function of SFLC. The Kalman filter is to reduce the physiologic and measurement disturbance of the vessel volume oscillation amplitude (VOA). The SFLC is composed of three parallel subcontrollers, each of which is a simple fuzzy logic controller, for processing the three changing states of the MAP: ascending, descending, and stabilizing states, respectively. The design of the fuzzy rules in each subcontroller is based on the *oscillometric principle* saying that the arterial vessel has the maximum compliance when the detected vessel volume pulse reaches its maximum amplitude. Simulation results show that, for the real physiologic MAP with changing rates up to 20 or −20 mm-Hg/minute, the model-based SFLC can beat-to-beat adjust the tonometer's chamber pressure to follow the tendency of MAP accurately.**

***Index Terms*—Blood pressure, compliance, oscillometry, tonometer, vessel volume pulse.**

I. Introduction

THE MODERN technologies of noninvasively automatic blood pressure measurement primarily include the Korotkoff and oscillometric methods. Both methods utilize an occlusive cuff, as an external pressure source, wrapping around a subject's upper arm to disclose the systolic and diastolic pressures within 30–60 s. In the oscillometric method, as the occluding cuff pressure is gradually reduced from above systolic values to below diastolic values, occlusive cuff pressure oscillations or vessel volume pulses show a specific pattern [1]–[4]. It is now generally accepted that *a maximum vessel volume pulse or occlusive cuff pressure oscillation occurs when the occlusive cuff pressure is equal to the mean arterial pressure* (MAP) [5]–[8]. This means that the artery can be considered to be in the *grossly unloading condition* between the artery and the cuff pressure.

A variety of techniques have been proposed to noninvasively register continuous arterial blood pressure waveform. Yamakoshi and others employed the vascular unloading technique to measure the continuous blood pressure from the arteries in fingers or heads [9]–[12]. In their instruments, there are two types of sensors, i.e., photocouple and pizeoresister transducer, that are used in the open loop control and the closed loop control individually. In the open loop control, the photocouple detected the subject's MAP and to keep the cuff pressure equal to the MAP. A shaker changed the cuff pressure to follow the intra-arterial pressure in the closed loop control. Since Stein and Blick first developed a mechanical force-sensing arterial tonometer, various kinds of tonometer using piezoresistive or strain gage pressure transducers have been designed to register the blood pressure waveform in the superficial artery [13]–[17]. These tonometric sensors may consist of an array of these pressure transducers to detect the correct position in the arterial vessel. But, they did not consider the problem that these force-sensors would change vessel compliance. As a result, a moderate accuracy was achieved when applying one of those tonometers. Another method is photoplethysmography which is constructed from a photocell and a light source to determine the blood flow in a limb by the measurement of volume changes of the limb. Therefore, it was used to detect the radial artery filling for a rapid noninvasive measurement of arterial opening pressure [18]. Drzewiecki *et al.* designed a flexible diaphragm tonometer to simultaneously measure arterial blood pressure waveform and vessel volume pulse with piezoresistive pressure transducer and impedance plethysmography [19]. This tonometric sensor was also placed at the superficial artery. Because these studies usually did not consider the coupling condition between the sensor and the arterial vessel in long term measurement, the accuracy of the measured blood pressure waveform with their devices was uncertain due to not taking the time-varying MAP into account.

Several control techniques have been implemented in the drug syringe to maintain the patient's MAP in the desired range [20]–[22]. These control schemes belong to the set-point ones, in which the plant has a target output for determining the error signal for the controller. Moreover, most of the previous control systems operated mainly on some mathematical models of

Manuscript received November 27, 2000; revised September 15, 2001. This work was supported by the National Science Council of Taiwan, R.O.C., under NSC Grant 90-2213-E009-103. This paper was recommended by Associate Editor V. B. Kolmanovskii.

S.-H. Liu is with the Department of Biomedical Engineering, Yuanpei Institute of Science and Technology, Hsinchu, 300 Taiwan, R.O.C. (e-mail: shliuymit@yahoo com.tw).

C.-T. Lin is with the Department of Electrical and Control Engineering, National Chiao-Tung University, Hsinchu, 300 Taiwan, R.O.C., (e-mail: ctlin@fnn.cn.nctu.edu.tw).

Publisher Item Identifier S 1083-4427(01)11300-7.

patients. However, it is difficult to identify a useful and simple mathematical model of patients due to the complexity of the human body. Even with an available mathematical model, it is still not easy to design a controller to meet the practical requirements. Recently, the fuzzy logic control (FLC) has been widely applied in the anesthesia control and other biomedical control [23]–[27]. One of the advantages in using the FLC is that it can be constructed empirically without explicit mathematical models of nonlinear physiological systems. Also, since the FLC is based on linguistic rules, it is not difficult to establish a measurement system with the FLC.

In order to measure the continuous blood pressure waveform accurately without distortion using a flexible diaphragm tonometer, the goal of this paper is to keep the tonometer's mean chamber pressure close to the MAP, i.e., to keep the *grossly unloading condition*, because the arterial vessel has the maximum compliance in this condition [3], [4], [8]. Since the MAP cannot be measured directly, we shall apply the *oscillometric principle* which indicates that if the detected vessel volume pulse can be kept at its maximum amplitude, the grossly unloading condition can be guaranteed [8], [19]. According to this principle, since the vessel volume pulse can be measured by the tonometer through the impedance method, the control objective in our measuring system is to keep the vessel volume pulse always at its maximum amplitude. However, the relationship between the amplitude of the detected vessel volume pulse and the difference of the mean chamber pressure and the MAP (i.e., the *transmural* pressure) is nonmonotonous quadratic-function-typed. Moreover, since the tendency of MAP always responses to human physiological conditions, it varies with time. Hence, when the detected vessel volume pulse departs from the maximum amplitude, the controller has no sense on the adjustment direction. What worse is that the real MAP waveform itself contains a large amount of physiologic disturbance inherently. Therefore, maintaining the grossly unloading condition is a *time-varying noisy trajectory-tracking control problem with unmeasureable desired trajectory* [28], which is a challenging task. To solve this problem, a Kalman filter is designed to reduce the physiologic and measurement disturbance of the VOA, and a linear predictor is designed to estimate the changing tendency of the MAP [29]–[33]. When the estimated MAP is increasing, the controller should increase the chamber pressure; otherwise, the controller should decrease the chamber pressure such that the vessel volume pulse can regain its maximum value. In this way, the grossly unloading condition can be maintained stably.

According to the approach proposed in the above, the proposed system for tracking the tendency of the MAP consists of a modified tonometer, a microsyringe device, a linear predictor, a Kalman filter, and a fuzzy controller. The tonometer can simultaneously measure the arterial blood pressure waveform and vessel volume pulse, and thus, through the microsyringe device, the changed vessel volume amplitude caused by the change of the MAP can be compensated by applying a counter pressure on the tonometer chamber to maintain the maximum vessel volume amplitude. A proposed synthetic fuzzy logic controller (SFLC) is used to control the microsyringe. The SFLC is composed of three parallel subcontrollers, each of which is a simple fuzzy logic controller, for processing the three changing states of the MAP: ascending, descending and stabilizing states, respectively. At the same time, a model-based linear predictor is utilized to estimate the MAPs changing tendency and trigger a suitable subcontroller of the SFLC corresponding to the ascending, descending or stabilizing state of the MAP.

In order to construct a reliable predictor and testing environment, we derive a mathematical model to describe the interaction between the tonometer and the artery. The continuous arterial blood pressure waveform and vessel volume pulse relative to different chamber pressures can be simultaneously simulated based on this model. Using these simulated data, a nonlinear model and an autoregressive exogenous (ARX) model are built to describe the static and dynamic arterial pressure–volume relationship, respectively [34], [35]. Based on these models, a MAP linear predictor is set up and tuned to beat-to-beat adjust the function of SFLC, and a Kalman filter is constituted to reduce the physiologic and measurement disturbance of the VOA. For the real physiologic MAP with changing rates up to 20 or -20 mm-Hg/min, the simulated results show the good estimation capability of the model-based linear predictor that can estimate the tendency of MAP and adapt the SFLC well. Such an estimation capability is rather robust to the real MAP with the physiologic disturbance phenomenon due to the mechanism of Kalman filter. Hence, the SFLC can successfully control the mean chamber pressure of the tonometer to achieve the grossly unloading coupling condition in the measuring process.

This paper is organized as follows. In Section II, the sensory device and the chamber-artery model are presented. In Section III, the model-based synthetic fuzzy logic controller is designed for the proposed measurement system. In Section IV, the practically experimental measurement for verifying the derived mathematical model, and the simulation results of the chamber pressure control based on the proposed measurement system using the model-based SFLC are presented. Conclusions are made in Section V.

II. Sensory and Chamber Pressure–Volume Models

In this section, a mathematical model related to the oscillometry is derived to describe the interaction between the tonometer and the artery. This model includes the mechanics of the tonometer, the arterial pressure pulse waveform, and the mechanics of the arterial wall. Based on this model, we then apply the oscillometric principle to derive a mathematical model for describing the time-variant arterial pressure–volume relationship under the use of tonometer. With these models, we can then design a controller to control the mean chamber pressure to follow the tendency of MAP for the measurement system of continuous arterial blood pressure waveform in Section IV.

A. Mathematical Oscillometric Model of the Tonometer

An arterial tonometer with a flexible diaphragm, modified from the previous studies [19], [36], is constructed to concurrently record the arterial blood pressure and the vessel volume pulse. The designed tonometer is made mainly of plexiglass,

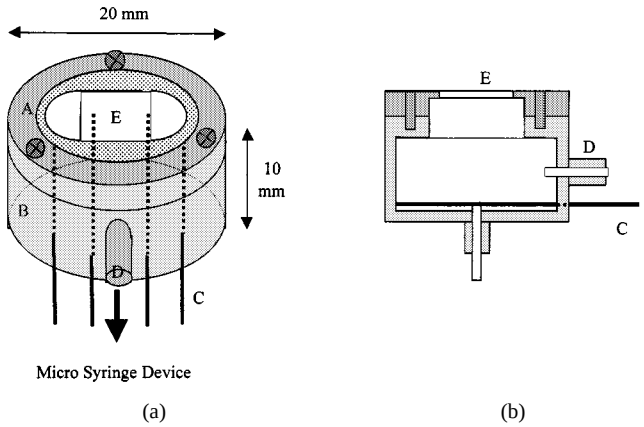

(a) (b)

Fig. 1. (a) Dimensional view of the modified flexible diaphragm arterial tonometer; (b) sectional view of flexible diaphragm tonometer. A, cover; B, main frame; C, four electrodes; D, water outlet, E, flexible diaphragm.

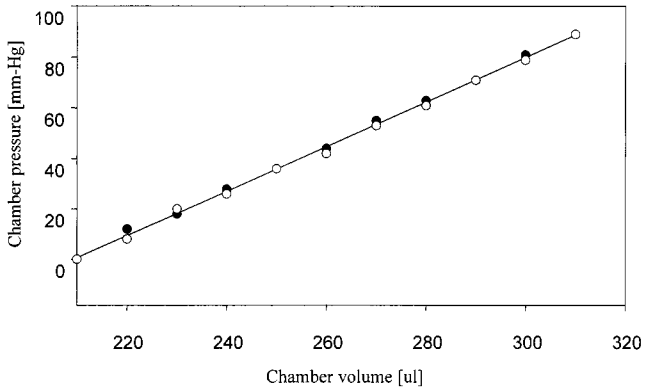

Fig. 2. Relationship between the chamber pressure and volume of the designed tonometer; where the empty circles represent the first measured pressure values, and the black circles represent the second measured pressure values.

and is miniaturized so that it could be directly placed over a superficial artery, as shown in Fig. 1. The change in the chamber pressure is continuously monitored using a pressure transducer (NPI-12, Lucas, USA) connected to the chamber. The variation of the vessel volume is assessed using the impedance plethysmography [19]. The relationship between the voltage difference, V_g, across the electrodes of the compartment and the volume of the compartment, V_m, can be expressed by

$$V_g = \frac{\rho I L^2}{V_m} \tag{1}$$

where I is the current passing through the compartment, ρ is the resistivity of the fluid in the compartment, and L is the length. It can be found that the more the volume, the smaller the voltage differences between the two electrodes. From Fig. 1, we also find that the tonometer can be considered as an air cuff bladder. Therefore, we adopted the oscillometric model of the cuff bladder to construct the oscillometric model of the tonometer.

Mechanics of Artery: In the blood pressure measurement, the cuff bladder and the tonometer are placed in different locations. Usually, the cuff bladder is utilized to detect the deep artery, like the brachial artery. Therefore, the cuff bladder fully makes the deformation of the vessel wall. Relatively, the tonometer is utilized to detect the superficial artery, like the radial artery. The flexible diaphragm only deforms the part of the vessel wall. However, since the radial bone is below the artery, the artery can also be considered to be in the fully compressed condition. Therefore, the vessel lumen is typically circular for positive transmural pressure. Oppositely, when the transmural pressure is negative, the lumen that will be compressed by the bone and the flexible diaphragm will deviate from a circular cross-section into an elliptical shape. This condition is like the variation of arterial cross-section in the oscillometric method. Therefore, in this paper, we adopt the vessel model and the arterial pressure pulse waveform function of Drzewiecki [7]. In the vessel model, the arterial distention follows a logarithmic function

$$A(t) = d \ln \frac{aP_t(t) + b}{1 + e^{-cP_t(t)}} \tag{2}$$

where A is the lumen area, $P_t(t)$ is the transmural pressure, and a, b, c, and d are the constants. Thus, the lumen's radius is

$$r(t) = \left(\frac{A(t)}{\pi}\right)^{0.5}. \tag{3}$$

A radial arterial pressure pulse, $P_a(t)$, is synthesized with the Fourier series:

$$P_a(t) = \text{MAP} + A_0 \sin(\omega_0 t) + A_1 \sin(2\omega_0 t) \tag{4}$$

where ω_0 is the heart rate, and A_0, A_1 are the Fourier coefficients. These constants are shown in the Table I.

Tonometer Model: To derive the tonometer model, we practically perform an experiment to obtain the pressure–volume relationship of the tonometer. In the beginning, the chamber is filled with saline from one outlet, and another outlet is used for the removal of the air. Then, one outlet is closed, and the chamber pressure is calibrated with the atmosphere pressure. We add more saline into the chamber, and record the relative chamber pressure until above 130 mm-Hg. Fig. 2 describes the relationship between the chamber pressure and volume. According to these results, the tonometer's flexible diaphragm deformation and stretch can be modeled by a linear function:

$$P_c(t) = y_0 + y_1 V_c(t) \tag{5}$$

where y_0 and y_1 are the coefficients of the linear regression in Fig. 2, $P_c(t)$ is the chamber pressure, and $V_c(t)$ is the chamber volume. Then, the transmural pressure can be obtained as follows:

$$P_t(t) = P_a(t) - P_c(t). \tag{6}$$

Radial Dynamic Model: Because the saline is uncompressible, we only need to consider the vessel lumen affecting the change of the chamber volume. Since the vessel length for measurement with the tonometer is constant, the vessel volume can be represented by a cross section. In order to calculate the lumen area easily, the lumen is considered to be in the circular shape. Fig. 3 shows three representative cases of relationship between the lumen and chamber in different transmural pressures, where the distance, d, from the lumen center to flexible diaphragm

TABLE I
CONTROL VALUES OF MODEL CONSTANTS

Parameters	Value	Units	Role
V_{co}	210	ul	Tonometer constants
w	4	mm	
L	6	mm	
y_0	-183.9	mm-Hg	
y_1	0.881	mm-Hg/ul	
D	0.4	mm	
a	0.03	mm-Hg^{-1}	Artery constants
b	3.3	non	
c	0.1	mm-Hg^{-1}	
d	0.08	cm	
MAP	100	mm-Hg	Arterial pressure
A_0	15	mm-Hg	waveform constants
A_1	9	mm-Hg	
f_{heart_rate}	80	beats/min	

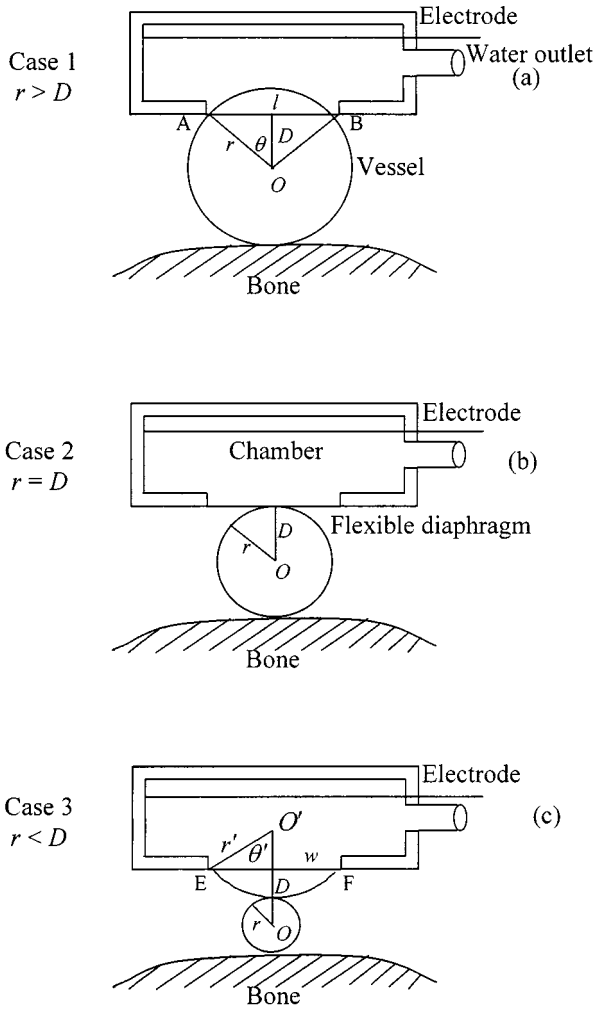

Fig. 3. Mechanical properties of the chamber and lumen volumes under different transmural pressures.

is constant. In Case 1, the transmural pressure is positive, so the lumen radius, r, is greater than the distance, D. Therefore, the flexible diaphragm is a concave. We can use the geometric method to calculate the lumen area inside the chamber. An included angle ($\angle$ AOB) is 2θ, and the chord of the arc is $l(t)$,

$$2\theta(t) = 2\cos^{-1}\left(\frac{D}{r(t)}\right) \tag{7}$$

$$l(t) = 2r\sin(\theta(t)). \tag{8}$$

Hence, the changed amount of chamber volume, $V_a(t)$, due to the stretching vessel lumen is

$$V_a(t) = L\left(r^2\theta(t) - 0.5Dl(t)\right) \tag{9}$$

where L is the measured lumen length. In Case 2, the transmural pressure is zero, so the lumen radius, r, is equal to the distance, D, and the volume, $V_a(t)$, is zero. In Case 3, the transmural pressure is negative, and r is smaller than D. Thus, the flexible diaphragm forms a protrudent shape, like a cambered surface with center point at $O'(t)$ and the radius being $r'(t)$, which is changed by the increased chamber volume and the change of the lumen cross-section. In this condition, the width of the measurement hole of the tonometer, w, is constant. Therefore, the protrudent volume of the flexible diaphragm, $V_{\rm pro}(t)$, can be calculated by the geometric method

$$r'(t) = 0.5(D - r(t)) + \frac{w^2}{8(D - r(t))} \tag{10}$$

$$2\theta'(t) = \cos^{-1}\left(\frac{r'(t) - (D - r(t))}{r'(t)}\right) \tag{11}$$

$$V_{\rm pro}(t) = L\left(r'(t)^2\theta'(t) - 0.5w\left(r'(t) + r(t) - D\right)\right) \tag{12}$$

where the included angle ($\angle$EO'F) is $2\theta'(t)$. The artery and the tonometer are interfaced via the protrudent volume of the flexible diaphragm, $V_{\rm pro}(t)$, whose change can be regarded as the change of the vessel lumen. Hence, the volume $V_a(t)$ is

$$V_a(t) = V_{\rm pro}(t) - V_{\rm pro}(t-1). \tag{13}$$

To simulate an actual arterial blood pressure and vessel volume change measurement procedure, the chamber volume is increased by slowly syringing saline into the chamber. Thus,

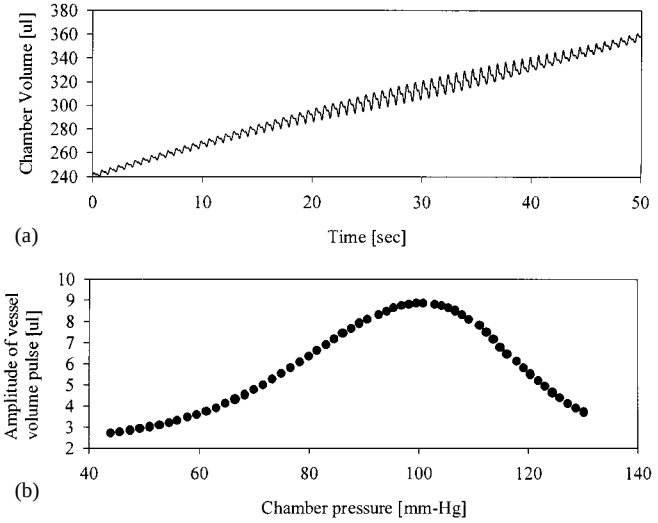

Fig. 4. Derivation of the static arterial pressure–volume relationship from the proposed tonometer's model. (a) Curve of the chamber volume in the pumping water process; (b) distribution of the vessel volume amplitude with respect to the chamber pressure.

the chamber volume, $V_c(t)$, is computed with both $V_a(t)$ and $V_i(t)$,

$$V_c(t) = V_{\rm co} + V_a(t) + V_i(t) \tag{14}$$

where $V_{\rm co}$ is the initial volume of the chamber, and $V_i(t)$ is the syringe volume whose increased rate is 3 ul/s. In Table I, we list all the constant values of the model. By relating the tonometer chamber pressure and volume to the arterial pressure and volume with (6), (9), and (13), (2), (5), and (14) can be solved simultaneously for the tonometer chamber pressure, $P_c(t)$, and volume, $V_c(t)$, at every instant of time. Because these equations are nonlinear, a computer solution is obtained using a numerical root-solving algorithm. Fig. 4 shows the simulation results of the tonometer model. The arterial blood pressure is preset at the MAP equal to 100 mm-Hg, systolic pressure at 121 mm-Hg, and diastolic pressure at 79 mm-Hg. Fig. 4(a) shows the oscillometric process of chamber volume. Because the alternating current amount of chamber volume is smaller than the direct current amount of chamber volume, we use a second-order high-pass filter whose cuff-off frequency locates at 0.5 Hz to filter the direct current amount of chamber volume. All amplitudes of the vessel volume pulses corresponding to each heartbeat are extracted and plotted with respect to the chamber pressure, as shown in Fig. 4(b).

B. Model of Chamber Pressure–Volume Relationship

In this section, we shall apply the oscillometric principle to derive a nonlinear-function-type model for modeling the time-variant arterial pressure–volume relationship under the use of the tonometer. Since the nonlinear model cannot completely describe the dynamic relationship between the chamber pressure and the vessel volume pulse, an autoregressive exogenous (ARX) model is further derived to model the dynamics of the tonometer [35].

1) Nonlinear Model: Because the tendency of MAP always responses to human physiological conditions, it varies with time. Fig. 4(b) shows that, the relationship between the chamber pressure and amplitude of vessel volume pulse is a nonlinear function. If the blood pressure pulse is constant, the MAP is the only time-variant variable in this function. Hence, by the curve fitting techniques, the envelope of the vessel volume oscillation amplitude, VOA, can be approximated by a nonlinear time-variant function which depends on the chamber pressure. Although, in Fig. 4(b), the envelop of VOA behaves as an asymmetric function, we only adopt a symmetric function to fit the envelope of VOA around its maximum amplitude to reduce the complexity of the model. This simplified model is good enough for our control propose since when the detected vessel volume pulse departs from the maximum amplitude, the controller must immediately change the chamber pressure to regain the new maximum amplitude to follow the MAP. Thus, a Gaussian curve which is represented by the solid line in Fig. 5 can be governed by the following equation:

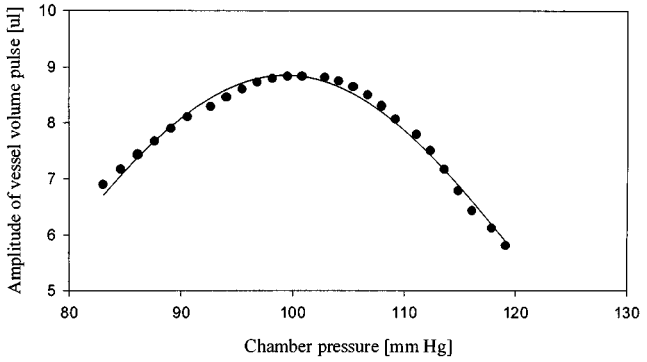

Fig. 5. Performance of the nonlinear regression model of the tonometer, $\mathrm{VOA}(t) = \mathrm{VOA}_{\max} e^{-0.5(P_c(t)-\mathrm{MAP}(t)/\sigma)^2}$, demonstrated by solid line, where the regression coefficient is 0.993, $\mathrm{VOA}_{\max}(t)$ is 8.85, $\mathrm{MAP}(t)$ is 99.4, and σ is 21.9. The dot curve shows the distribution of the vessel volume amplitude, which is part of the curve in Fig. 4(b) around its maximum amplitude.

$$\mathrm{VOA}(t) = \mathrm{VOA}_{\max} e^{-0.5(P_c(t)-\mathrm{MAP}(t)/\sigma)^2} \tag{15}$$

where σ is a constant and $\mathrm{VOA}_{\max}$ is the maximum of VOA.

2) Dynamic Model: The relationship between the vessel volume and transmural pressure was formulated as a static nonlinear mapping in Section IV-B. In this section, we shall consider the dynamic model of the vessel volume oscillation amplitude that describes the pumping process in the coupling condition between the chamber pressure and the arterial pressure. This nonlinear black-box model can be represented by a single-input/single-output time-variant ARX model

$$\mathrm{VOA}(t) = -\sum_{i=1}^{n_a} a_i(t)\mathrm{VOA}(t-i) + \sum_{j=1}^{n_b} b_j(t)P_c(t-j) + \varepsilon(t) \tag{16}$$

where t denotes the discrete time step, $\varepsilon(t)$ is the residual error, n_a and n_b represent the number of the model order, and a_i and b_j are the time-variant coefficients of the model. From Fig. 4(a), we find that the procedure of pumping saline into the chamber only needs a short time, about 50 s. Hence, we assume that the evolution of the MAP tendency is so slow, such that in the cycle of

creating dynamical model, the MAP is considered as a constant value. In this case, the time-variant ARX model will be reduced to the time-invariant ARX model as the following equation:

$$\mathrm{VOA}(t) = -\sum_{i=1}^{n_a} a_i \mathrm{VOA}(t-i) + \sum_{j=1}^{n_b} b_j P_c(t-j) + \varepsilon(t). \quad (17)$$

We use a linear regression method to create the ARX model [35]. The regression vector, $\phi(t)$, and the parameter vector, θ, are introduced in (18) and (19), shown at the bottom of the page. Therefore, we can rewrite (17) as a linear regression model

$$\mathrm{VOA}(t) = \phi^T(t)\theta + \varepsilon(t) \quad (20)$$

For each data segment, the parameter vector of the model is determined using a least-squares method. Let $\bar{\theta}$ denote an arbitrary estimate of the parameter vector θ. Then the loss function is defined as

$$V(\bar{\theta}) = \frac{1}{2} \sum_{t=l+1}^{N} \varepsilon(t)^2 \quad (21)$$

where N is the beat number in the increasing pressure process, and $l = \max\{n_a \; n_b\}$. An optimal estimate $\hat{\theta}$ of the parameter vector θ can be found from the measurement data, $\{\mathrm{VOA}(t)\}_{t=l+1}^{N}$ and $\{\phi(t)\}_{t=l+1}^{N}$, by minimizing the loss function $V(\bar{\theta})$:

$$\hat{\theta} = \left(\sum_{t=l+1}^{N} \phi(t)\phi(t)^T \right)^{-1} \sum_{t=l+1}^{N} \phi(t)\mathrm{VOA}(t). \quad (22)$$

The order of model, l, determines the complexity and accuracy of the model. While a too low-order model might not represent the actual dynamic system accurately, a too high-order model might easily incorporate noise i.e., overfitting and results in poor prediction capability. Therefore, the model validation is required to verify that the identified model fulfills the modeling requirements according to subjective and objective criteria of good model approximation. In this paper, (21) is used to determine the model order. Fig. 6 shows the base 10 logarithm of the $N-l$ points of the loss function values, $\log_{10}\left(V\left(\bar{\theta}\right)/N-l\right)$, in (21) with respect to the model order number, where the solid line corresponds to the clean VOA, and the dot line to the noisy VOA. The figure shows that these two curves overlap closely when the order number is below 10, and deviate gradually when the order is increasing. This means that the model reaches a good approximation capability at order 10, but is becoming overfitting at order larger than 10. From the above analysis, the model order chosen in our system in (17) is $n_a = n_b = 10$.

Fig. 6. Determining the optimal order of the ARX model, where solid line represents the base 10 logarithm of the $N-l$ points of loss function values in (21) without disturbance; dot line represents the corresponding loss function values with disturbance.

III. Model-Based Synthetic Fuzzy Logic Control (SFLC)

In normal control systems, the difference between the measured output and the desired output is used as the feedback to the controller, controlling the plant to achieve the level of the desired output [21], [23], [24], the so-called "set-point control". According to the optimal coupling condition and the oscillometric principle mentioned in Section II, since the vessel volume pulse can be measured by the tonometer, the goal of our controller is to keep the vessel volume pulse at its maximum amplitude. An obvious dilemma to this control goal is that the maximum amplitude to be reached is *changing from time to time and is unknown in advance*. Hence, what we meet is the time-varying trajectory tracking control problem with unknown desired trajectory. From Fig. 5, if the chamber pressure is greater or lower than the present MAP, the amplitude of vessel volume pulse will become smaller than the maximum. Moreover, since how the subject's MAP varies in each heartbeat and whether the tendency of MAP is in the ascending or descending state are unknown, the controller cannot utilize the difference information to regulate the chamber pressure. What worse is that the real MAP waveform itself contains a large amount of physiologic disturbance inherently. Therefore, in this section, a Kalman filter is used to reduce the physiologic disturbance of MAP, and a model-based synthetic fuzzy logic controller (SFLC) is designed to control the chamber pressure. The model-based SFLC consists of the SFLC and a model-based linear predictor. The SFLC can control the measurement system under three different changing states of the MAP, and the model-based linear predictor can estimate the MAPs changing tendency to adjust the SFLC properly.

A. Kalman Filter

In designing a controller to beat-to-beat adjust the chamber pressure following the MAP, two disturbance factors should be

$$\phi^T(t) = [-\mathrm{VOA}(t-1) \ldots -\mathrm{VOA}(t-n_a) \quad P_c(t-1) \ldots P_c(t-n_b)], \quad (18)$$

$$\theta^T = [a_1 \ldots a_{n_a} \quad b_1 \ldots b_{n_b}]. \quad (19)$$

considered. First, the MAP is not a constant in each beat, although it still maintains in a physiologically stabilized state. The other is the quiver of the measured hand in the measurement process. To overcome these disturbances, we consider the measurement of VOA as a state-estimation problem and perform the recursive estimation of the state with the aid of the Kalman filter [29], [37]. For this, we need to prepare our model in the state-space form consisting of two jointed linear equations: the state equation and the observation equation. More precisely, we rewrite the ARX model in (17) as follows:

$$x(t+1) = Ax(t) + Bu(t) + We(t+1) \tag{23}$$

$$y(t) = Cx(t) + e(t) \tag{24}$$

where the state is $x(t) = [\mathrm{VOA}(t-n_a) \ldots \mathrm{VOA}(t-1)]^T$, the input vector is $u(t) = [P_c(t-1) \ldots P_c(t-n_b)]^T$, the measurement errors are $e(t)$, $e(t-1)$, and the system matrices are

$$A = \begin{bmatrix} 0 & 1 & 0 & \ldots & 0 \\ 0 & 0 & 1 & \ldots & 0 \\ \vdots & & & \ddots & \vdots \\ 0 & 0 & 0 & & 1 \\ -a_{n_a} & -a_{n_a-1} & & \ldots & -a_1 \end{bmatrix} \tag{25}$$

$$B = \begin{bmatrix} 0 & \ldots & 0 \\ \vdots & \ddots & \vdots \\ b_1 & \ldots & b_{n_b} \end{bmatrix} \tag{26}$$

$$W = [0 \quad \ldots \quad 1]^T, \qquad C = [0 \quad \ldots \quad 1]. \tag{27}$$

We will make the assumption that the covariances of the state and observation processes are diagonal and time invariant, i.e., $\Omega_e(t) = E\left[e(t)e(t)^T\right] = \sigma_e^2 I$.

Based on the model output and the previous signal measurement, the optimal mean square error estimate $\hat{\mathrm{VOA}}(t)$ of $\mathrm{VOA}(t)$ [38]. According to the Kalman filter theory, the system state can be recursively estimated by

$$\hat{x}(t+1) = A\left\{\hat{x}(t) + K(t)\left[y(t) - C\hat{x}(t)\right]\right\} + Bu(t) \tag{28}$$

where the gain $K(t)$ is obtained by Kalman recursion:

$$R(t) = AP(t)A^T + W\Omega_e(t+1)W^T \tag{29}$$

$$K(t) = R(t)C^T\left[CR(t)C^T + \Omega_e(t)\right]^{\iota}, \tag{30}$$

$$P(t+1) = [I - K(t)C]R(t) \tag{31}$$

where $(\bullet)^{\iota}$ denotes the pseudo-inverse. Using the above equations, an estimated $\hat{\mathrm{VOA}}(t) = C\hat{x}(t+1)$ can be obtained after each observation of $\mathrm{VOA}(t)$, and the respective chamber pressure, $P_c(t)$, can be calculated via (28)–(31).

B. Model-Based Linear Predictor

In Section III-A, we have derived the chamber-artery nonlinear time-variant model of tonometer in (15). This model is used here to identify the varying situations of the MAP [35]. The goal is to predict the changing tendency of the MAP; i.e., to identify whether the MAP is in ascending, stabilization, or descending state. To achieve this goal, we shall design a linear predictor to predict the value of MAP at the time step t, $\hat{\mathrm{MAP}}(t)$, such that the difference between the corresponding $\hat{\mathrm{VOA}}(t)$ and the real $\mathrm{VOA}_{\max}$ is minimum. In other words, the least square criterion for tuning the linear predictor based on the time t sample is

$$E\left(\hat{\mathrm{MAP}}(t)\right) = \frac{1}{2}\left[\mathrm{VOA}_{\max} - \hat{\mathrm{VOA}}(t)\right]^2 = \frac{1}{2}\varepsilon(t)^2\left(\hat{\mathrm{MAP}}(t)\right) \tag{32}$$

where $\hat{\mathrm{VOA}}(t)$ is the estimated amplitude by the Kalman filter when the model's parameter is $\hat{\mathrm{MAP}}(t)$, and $\varepsilon(t) = \left(\mathrm{VOA}_{\max} - \hat{\mathrm{VOA}}(t)\right)$ is the prediction error. Taking the gradient of the optimization criterion in (32) can do the least criterion

$$\frac{\partial E\left(\hat{\mathrm{MAP}}(t)\right)}{\partial \hat{\mathrm{MAP}}(t)} = \frac{1}{\sigma}\varepsilon(t)\hat{\mathrm{VOA}}(t)\left(P_c(t) - \hat{\mathrm{MAP}}(t)\right). \tag{33}$$

Therefore, the recursive linear predictor using the gradient is described by

$$\hat{\mathrm{MAP}}(t+1) = \hat{\mathrm{MAP}}(t) + \frac{g}{\sigma}\varepsilon(t)\hat{\mathrm{VOA}}(t)\left(P_c(t) - \hat{\mathrm{MAP}}(t)\right) \tag{34}$$

where g is the constant gain. Here, we use the gradient of $\hat{\mathrm{MAP}}(t)$ as the decision value. If a decision value falls within a threshold region, it means that the present MAP is in a stable state. Thus, the decision maker will trigger the Stabilizing FLC in the SFLC to keep the chamber pressure. However, if a decision value is beyond the threshold region, it implies that the MAP is ascending or descending now, so the decision maker will activate either the Ascending FLC or Descending FLC in the SFLC.

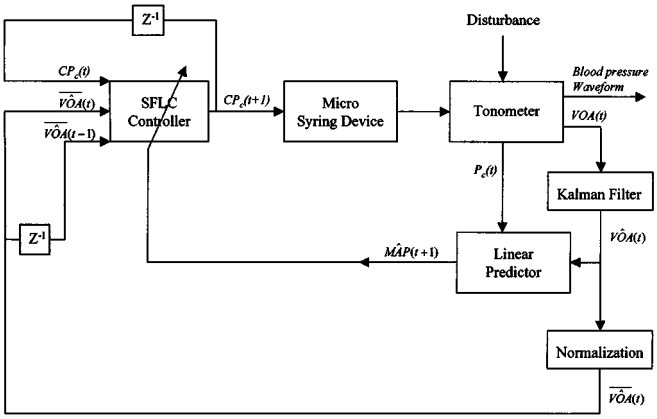

Fig. 7. Block diagram of the closed-loop chamber pressure control of the proposed measurement system.

C. Synthetic Fuzzy Logic Controller (SFLC)

Fig. 7 shows the block diagram of the close-loop chamber pressure control of the proposed measurement system. The whole system consists of a SFLC, a Kalman filter used to reduce the disturbances that are produced by the MAP's

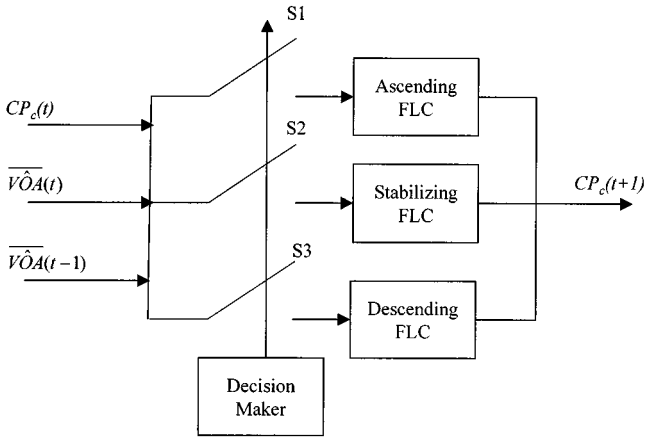

Fig. 8. Structure of the proposed synthetic fuzzy logic controller (SFLC) that includes the ascending, descending, and stabilizing subcontrollers, and a decision maker.

physical phenomenon and the environmental effect, a linear predictor used to adjust the SFLC, a microsyringe device used to change the chamber pressure of the tonometer, and proper disturbance added to the simulation model to create a more realistic control environment. The tendency of the MAP is quite stable in normal situations, but it is likely that a great change in MAP occurs due to blood pressure-related diseases or other intervention. In accordance with these reasons, the designed SFLC is composed of three parallel subcontrollers, i.e., the Ascending FLC, Stabilizing FLC, and Descending FLC, as shown in Fig. 8. A decision maker enables one of the three subcontrollers based on the estimation result of the linear predictor that is used to beat-to-beat estimate the changing tendency of MAP.

In the beginning, we create the nonlinear model and dynamic model of the chamber pressure–volume, then adapt the chamber pressure until the oscillation amplitude of vessel volume reaches its maximum $\mathrm{VOA}_{\max}$. The measured $\mathrm{VOA}(t)$ and the related chamber pressure, $P_c(t)$, pass the Kalman filter to obtain the more truthful estimated $\hat{\mathrm{VOA}}(t)$. It will be used to estimate the rough tendency of the MAP by the linear prediction. At the same time, it is also normalized and used as the SFLCs input. The SFLC designed here requires three input variables. They are the current and preceding estimated normalized oscillation amplitude of vessel volume, $\overline{\hat{\mathrm{VOA}}}(t)$ and $\overline{\hat{\mathrm{VOA}}}(t-1)$, and the amount of change in the chamber pressure, $CP_c(t)$. The output of the SFLC, $CP_c(t+1)$, is used to trigger the microsyringe device, modulating the chamber pressure. Here, $t-1$ and $t+1$ indicate the preceding and the next sampling time of t, respectively.

The three parallel subcontrollers in the SFLC possess the similar fuzzifiers and defuzzifiers, but have different rule bases. In either of the Ascending and Descending FLCs, the fuzzy term set for $CP_c(t)$ is composed of nine membership functions: much push (MP), moderately push (DP), little push (LP), very little push (VLP), zero (Z), very little draw (VLD), little draw (LD), moderately draw (DD), and much draw (MD). These fuzzy terms are defined by means of triangular functions in the $[-2.04\ 2.04]$ subset of real numbers. The current or preceding estimated normalized oscillation amplitude of vessel volume, $\overline{\hat{\mathrm{VOA}}}(t)$ or $\overline{\hat{\mathrm{VOA}}}(t-1)$, determines the degree of the coupling between the vessel's side and the tonometer's side with five membership functions, defined in the [0.954 1] subset of real numbers: BEST, BETTER, GOOD, WORSE, and WORST. In the Stabilizing FLC, the fuzzy terms of $\overline{CP_c}(t)$ are defined in $[-1.86\ 1.86]$, and those of $\overline{\hat{\mathrm{VOA}}}(t)$ and $\overline{\hat{\mathrm{VOA}}}(t-1)$ are defined in [0.972 1].

The representative fuzzy rules for the Ascending, Descending, and Stabilizing FLCs are as follows, respectively:

```
THE ASCENDING FLC:
 WHEN CP_c(t) is Z,
 IF VOA^(t) is BETTER and VOA^(n-1) is BEST,
 THEN CP_c(t+1) is VLP.
THE DESCENDING FLC:
 WHEN CP_c(t) is Z,
 IF VOA^(t) is BETTER and VOA^(t-1) is BEST,
 THEN CP_c(t+1) is VLD.
THE STABILIZING FLC:
 WHEN CP_c(t) is VLD,
 IF VOA^(t) is GOOD and VOA^(t-1) is BETTER,
 THEN CP_c(t+1) is VLP.
```

The meaning of the above rules is explained as follows. If a smaller $\overline{\hat{\mathrm{VOA}}}(t)$ is yielded, the Ascending FLC will trigger the microsyringe device to elevate the chamber pressure since the Ascending FLC is activated by the decision maker when the MAP is in the ascending state, i.e., in the direction of approaching its maximum. On the contrary, if a smaller $\overline{\hat{\mathrm{VOA}}}(t)$ is observed, the Descending FLC will decrease the chamber pressure, since the Descending FLC is activated when the MAP is in the descending state, i.e., in the direction of departing from its maximum. Therefore, the functions of the rules in the Ascending FLC are opposite to those in the Descending FLC. In the above fuzzy rule of the Stabilizing FLC, if the chamber pressure is increased at time t, and an attenuated amount of $\overline{\hat{\mathrm{VOA}}}(t)$ is found to be larger than that of $\overline{\hat{\mathrm{VOA}}}(t-1)$, then this control action is incorrect. Thus, it is required to trigger the microsyringe device to reduce the chamber pressure at the next time step, $t+1$. Basically, the rule structure of the Stabilizing FLC is itself symmetric.

The individual-rule-based inference process is supervised by computing the degree of match between the fuzzified input values and the fuzzy sets describing the meaning of the rule-antecedent, as described in the rule set. The Mamdani's max-min operator [39] is used to find the possibility distribution function. The technique of 'center of area' is used to process the defuzzification and to calculate the output, $CP_c(t+1)$, of the controllers.

IV. Experiment and Simulation Results

A. Experiment Process

In this section, we practically use the designed tonometer to measure one subject (male, 22 years, systolic/diastolic/mean

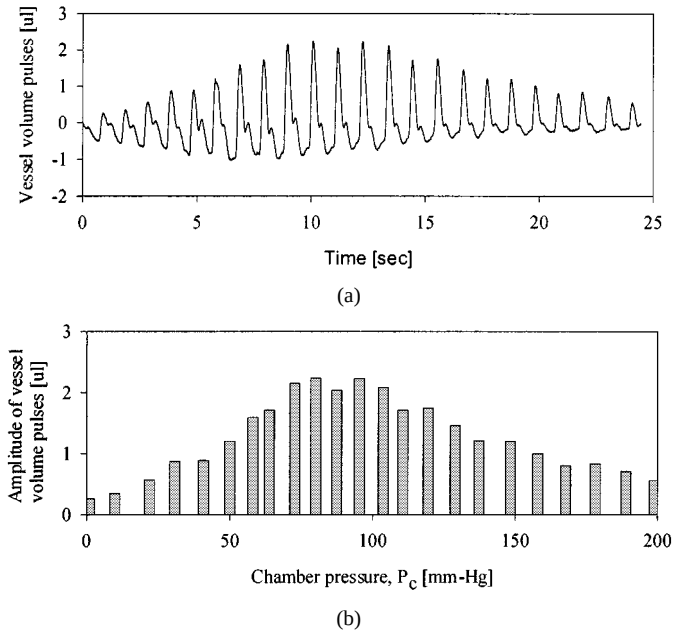

Fig. 9. Derivation of the static arterial pressure–volume relationship from a test subject. (a) Curve of the vessel volume pulse versus the chamber pressure; (b) distribution of the vessel volume amplitude with respect to the chamber pressure.

pressure being 112/76/89 mm-Hg) with normotension, and record the vessel volume amplitudes corresponding to different chamber pressures. From this experiment, we can check the validity of the mathematical oscillometric model of tonometer derived in Section II-A. The modified tonometer was placed over the radial artery of the subject and fixed with elastic bandage. The chamber pressure of the tonometer was gradually increased up to 160 mm-Hg, at a rate of 3 mm-Hg/s by means of the controlled microsyringe device. A period of 30-s measured signal of the chamber pressure and vessel volume pulse was digitized with a sampling frequency of 100 Hz and recorded using the A/D card (ADVANTEC PCL 818 LG) based on Pentium 133 personal computer. Fig. 9 shows the static arterial pressure–volume relationship. Fig. 9(a) shows the curve of the vessel volume pulses yielded by high-pass filtering the original measured signal of vessel volume. All amplitudes of the vessel volume pulses corresponding to each heartbeat are extracted and plotted with respect to the chamber pressure, as shown in Fig. 9(b). It can be seen that a peak occurs when the chamber pressure is close to the MAP. It is observed that the oscillometric phenomenon showing Fig. 9(b) is very close to that in Fig. 4(b), meaning that the mathematical oscillometric model of tonometer describes the practical system very well.

B. Simulation Results

Based on the data obtained in the above, we modeled the arterial pressure–volume relationship by (15), in which the value $\mathrm{VOA}_{\max}$ is 8.85, σ is 21.9 mm-Hg, and the MAP is 100 mm-Hg. In order to test the generalization capability of the SFLC, the chamber pressure was controlled to follow the desired MAP with a changing rate of ± 20 mm-Hg/min. In the linear predictor of our control system, the threshold region was chosen to be ± 0.1 mm-Hg through trial-and-error testing to obtain the

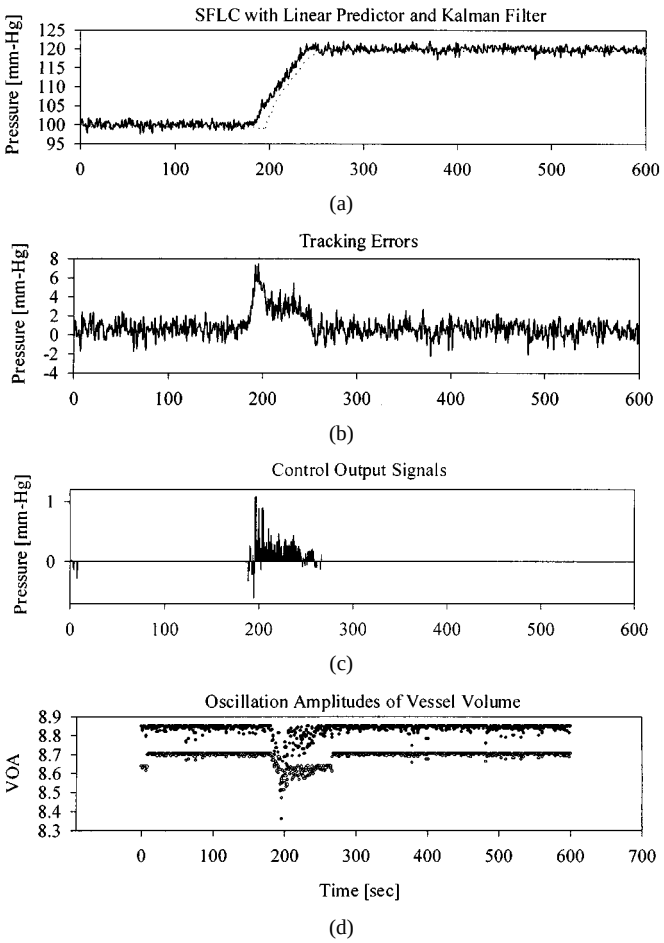

Fig. 10. Simulation results of the SFLC with a model-based linear predictor and a Kalman filter for tracking the tendency of MAP with a changing rate of 20 mm-Hg/min. (a) The desired MAP values with disturbance (solid line) and the chamber pressure $(P_c(t))$ under control (dot line); (b) the tracking error between the desired MAP and $P_c(t)$; (c) the SFLCs output signals; (d) the $\mathrm{VOA}(t)$ values (circle) and $\hat{\mathrm{VOA}}(t)$ values (empty circle).

best performance of the SFLC. In our simulations, the rate of the added disturbance to the variation of MAP in each heartbeat was set at about 1 mm-Hg.

Fig. 10 shows the control performance of the SFLC with a Kalman filter and a linear predictor, where the MAP is ascending and the changing rate is about 20 mm-Hg per minute. The chamber pressure under the SFLC control as well as the desired tendency of the MAP is shown in Fig. 10(a). It is observed that the chamber pressure follows the desired tendency of the MAP closely. To see the control performance more precisely, Fig. 10(b) shows the difference between the actual chamber pressure and the desired MAP. It is found that the tracking error is kept within a fixed amount that is about 3 mm-Hg when the MAP is ascending. When the tendency of the MAP becomes increasing, the controller has a transient duration with large error. The SFLC output signals are shown in Fig. 10(c). The SFLC output signals usually keep the pressure values positive in the ascending process. The SFLC produces only small positive or negative output signals to keep the vessel volume at its maximum in the stabilizing state. Fig. 10(d) shows the performance of the Kalman filter. We can find that the variation of $\hat{\mathrm{VOA}}(t)$ is smaller than that of $\mathrm{VOA}(t)$, showing that, the Kalman filter

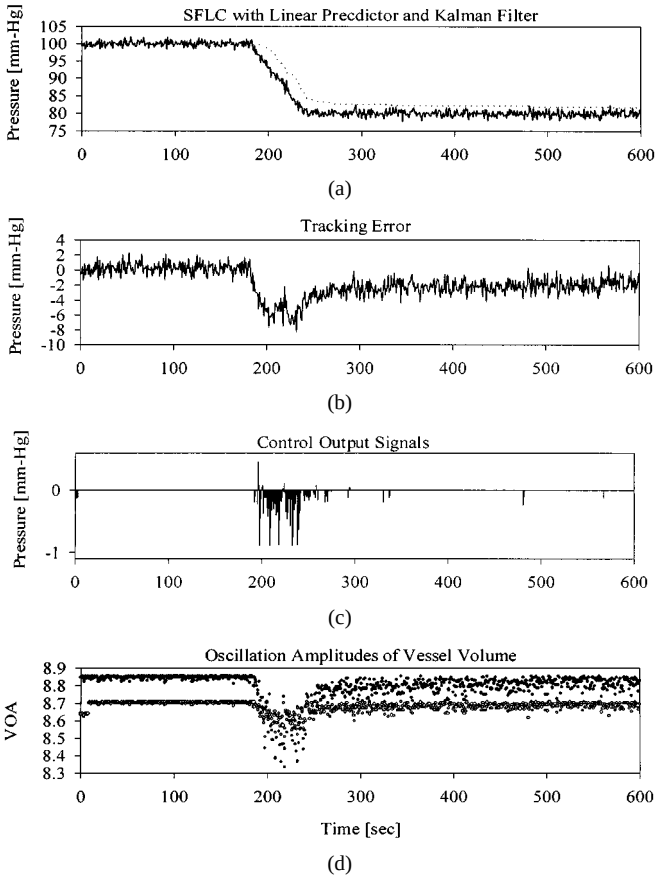

Fig. 11. Simulation results of the SFLC with a model-based linear predictor and a Kalman filter for tracking the tendency of MAP with a changing rate of -20 mm-Hg/min. (a) The desired MAP values with disturbance (solid line) and the chamber pressure ($P_c(t)$) under control (dot line); (b) the tracking error between the desired MAP and $P_c(t)$; (c) the SFLCs output signals; (d) the $\mathrm{VOA}(t)$ values (circle) and $\hat{\mathrm{VOA}}(t)$ values (empty circle).

is an efficient method to reduce the interference caused by the internal or external disturbance. Fig. 11 shows the control performance of the SFLC when the MAP is descending and the changing rate is about 20 mm-Hg per minute. From Fig. 11(b), we find that the tracking error is about 5 mm-Hg in the descending segment, but in the stabilizing state, the tracking error is only about 2 mm-Hg. There are two reasons for this larger tracking error. First, the fuzzy inference in SFLC is designed to firstly guess the ascending state, so if the guess is wrong, it will then try the against direction. Second, the parameter σ in (15) is large, but the error of the normalized amplitude of vessel volume pulse is only about 10^{-2}. Therefore, when the tracking error is decreased to about 2 mm Hg, the controller will not adjust the chamber pressure. Hence, if we can increase the resolution of the fuzzy term sets of $\overline{\hat{\mathrm{VOA}}}(n)$ and $\overline{\hat{\mathrm{VOA}}}(n-1)$, the tracking error is expected to be further reduced.

V. Conclusions

The results obtained in this study clearly indicate that the tonometric oscillometry with the impedance plethysmography permits the accurate identification of the MAP when it makes a large change due to blood pressure-related diseases or other intervention. This method, unlike another conventional continuous blood pressure measurement, is designed to measure blood pressure by detecting arterial volume pulsation and making a grossly unloading condition between the artery and the tonometer. Yamakoshi *et al.* did consider the unloading problem [9]–[12], but they didn't determine this condition when the MAP had a large amount of change on a danger illness. The conventional tonometers used only one transducer in the measurement [13]–[17], so they could not process the unloading problem. Drzewiecki designed a flexible diaphragm tonometer that used two sensors, including impedance plethysmography and pizeoresister transducer [19]. Because their goal was to measure the arterial vessel compliance, their system didn't have a controller to maintain the grossly unloading condition.

According above comparisons, this paper proposes the use of fuzzy logic control, called model-based synthetic fuzzy logic controller (SFLC), for achieving the grossly unloading condition in the noninvasive blood pressure measurement. The characteristics of the tonometer's mechanism have been analyzed to successfully simulate the changing situation of the chamber pressure and volume. The simulated data describing the continuous chamber pressure and changing volume waveforms were used to derive a nonlinear model and a dynamic model. In the nonlinear model, by applying the curve-fitting technique on the experiment data, a Gaussian function was adopted to model the relationship of the oscillation amplitude of vessel volume to the transmural pressure. Based on this model, a linear predictor was set up to estimate the MAP trajectory in each heartbeat, and the estimated results were feedback to the SFLC for choosing a proper subcontroller. In the dynamic model, we used the linear regression method to build an ARX model representing the dynamic relationship between the vessel volume oscillation amplitude and chamber pressure. A Kalman filter was used to estimate $\hat{\mathrm{VOA}}(t)$ with the measured $\mathrm{VOA}(t)$ and $P_c(t)$. This filter greatly reduced the disturbance to $\mathrm{VOA}(t)$. The simulation results showed that the SFLC with three parallel subcontrollers and a model-based linear predictor was capable of precisely controlling the chamber pressure to closely follow the time-varying tendency of the MAP. Since the whole control process is rather time efficient, the proposed control system can beat-to-beat control the chamber pressure in real time. Further clinical testing is needed to verify these conclusions practically.

References

[1] M. Ursino and C. Cristalli, "Mathematical modeling of noninvasive blood pressure estimation techniques—Part I: Pressure transmission across the arm tissue," *ASME J. Biomech. Eng.*, vol. 117, pp. 107–116, 1995.

[2] ——, "Mathematical modeling of noninvasive blood pressure estimation techniques—Part II: Brachial hemodynamics," *ASME J. Biomech. Eng.*, vol. 117, pp. 117–126, 1995.

[3] ——, "A mathematical study of some biomechanical factors affecting the oscillometric blood pressure measurement," *IEEE Trans. Biomed. Eng.*, vol. 43, pp. 761–778, 1996.

[4] F. K. Forster and D. Turney, "Oscillometric determination of diastolic, mean and systolic blood pressure—A numerical model," *ASME J. Biomech. Eng.*, vol. 108, pp. 359–364, 1986.

[5] L. A. Geddes, M. Voelz, C. Combs, D. Reiner, and C. F. Babbs, "Characterization of the oscillometric method for measuring indirect blood pressure," *Ann. Biomed. Eng.*, vol. 10, pp. 271–280, 1982.

[6] G. W. Mauck, C. R. Smith, L. A. Geddes, and J. D. Bourland, "The meaning of the point of maximum oscillations in cuff pressure in the indirect measurement of blood pressure—Part II," *ASME J. Biomech. Eng.*, vol. 102, pp. 28–33, 1980.

[7] G. Drzewiecki, R. Hood, and H. Apple, "Theory of the oscillometric maximum and the systolic and diastolic detection ratios," *Ann. Biomed. Eng.*, vol. 22, pp. 88–96, 1994.
[8] P. D. Baker, D. R. Westenskow, and K. Kuck, "Theoretical analysis of noninvasive oscillometric maximum amplitude algorithm for estimating mean blood pressure," *Med. Biol. Eng. Comput.*, vol. 35, pp. 271–278, 1997.
[9] K. Yamakoshi, H. Shimazu, and T. Togawa, "Indirect measurement of instantaneous arterial blood pressure in the human finger by the vascular unloading technique," *IEEE Trans. Biomed. Eng.*, vol. BME-27, pp. 150–155, 1980.
[10] K. Yamakoshi, H. Shimazu, and A. Kamiya, "New oscillometric method for indirect measurement of systolic and mean arterial pressure in the human finger. Part 2: Correlation study," *Med. Biol. Eng. Comput.*, vol. 20, pp. 314–318, 1982.
[11] K. Yamakoshi, A. Kamiya, H. Shimazu, H. Ito, and T. Togawa, "Noninvasive automatic monitoring of instantaneous arterial blood pressure using the vascular unloading technique," *Med. Biol. Eng. Comput.*, vol. 21, pp. 557–565, 1983.
[12] S. Tanaka and K. Yamakoshi, "Ambulatory instrument for monitoring indirect beat-to-beat blood pressure in superficial temporal artery using volume-compensation method," *Med. Biol. Eng. Comput.*, vol. 34, pp. 441–447, 1996.
[13] P. D. Stein and E. F. Blick, "Arterial tonometry for the atraumatic measurement of arterial blood pressure," *J. Appl. Physiol.*, vol. 30, pp. 593–596, 1971.
[14] T. Sato, M. Nishinaga, A. Kawamoto, T. Ozawa, and H. Takatsuji, "Accuracy of a continuous blood pressure monitor base on arterial tonometry," *Hypertension*, vol. 21, pp. 866–874, 1993.
[15] G. Drzewiecki, J. Melbin, and A. Noordergraaf, "Arterial tonometry: Review and analysis," *J. Biomech.*, vol. 16, pp. 141–152, 1983.
[16] G. Drzewiecki, "Noninvasive assessment of arterial blood pressure and mechanics," in *The Biomedical Engineering Handbook*, J. Bronzino, Ed. Boca Raton, FL: CRC, 1995, ch. 73, pp. 1196–1211.
[17] L. C. Siegel, J. G. Brock-Utne, and J. B. Brodsky, "Comparison of arterial tonometry with radial artery catheter measurements of blood pressure in anesthetized patients," *Anesthesiology*, vol. 81, no. 3, pp. 578–584, 1994.
[18] R. P. Schnall, N. Gavriely, S. Lewkowicz, and Y. Palti, "A rapid noninvasive blood pressure measurement method for discrete value and full waveform determination," *Amer. Physiol. Soc.*, pp. 307–314, 1996.
[19] G. Drzewiecki, B. Solanki, J. J. Wang, and J. K. Li, "Noninvasive determination of arterial pressure and volume using tonometry," in *Proc. IEEE-EMBS Conf.*, 1996, pp. 61–64.
[20] J. F. Martin, A. M. Schneider, M. L. Quinn, and N. T. Smith, "Improved safety and efficacy in adaptive control of arterial blood pressure through the use of a supervisor," *IEEE Trans. Biomed. Eng.*, vol. 39, pp. 381–388, 1992.
[21] C. Yu, R. J. Roy, H. Kaufman, and B. W. Bequette, "Multiple-model adaptive predictive control of mean arterial pressure and cardiac output," *IEEE Trans. Biomed. Eng.*, vol. 39, pp. 765–777, 1992.
[22] G. Jee and R. J. Roy, "Adaptive control of multiplexed closed-circuit anesthesia," *IEEE Trans. Biomed. Eng.*, vol. 39, pp. 1071–1080, 1992.
[23] H. Ying, M. Mceachern, D. W. Eddleman, and L. C. Sheppard, "Fuzzy control of mean arterial pressure in postsurgical patients with sodium nitroprusside infusion," *IEEE Trans. Biomed. Eng.*, vol. 39, pp. 1060–1070, 1992.
[24] J. W. Huang and R. J. Roy, "Multiple-drug hemodynamic control using fuzzy decision theory," *IEEE Trans. Biomed. Eng.*, vol. 45, pp. 213–228, 1998.
[25] D. A. Linkens, J. S. Shieh, and J. E. Peacock, "Hierarchical fuzzy modeling for monitoring depth of anesthesia," *Fuzzy Sets Syst.*, vol. 79, pp. 43–57, 1996.
[26] C. M. Held and R. J. Roy, "Multiple drug hemodynamic control by means of a supervisory fuzzy rule based adaptive control system: Validation on a model," *IEEE Trans. Biomed. Eng.*, vol. 42, pp. 371–385, 1995.
[27] J. W. Huang, Y. Y. Lu, A. Nayak, and R. J. Roy, "Depth of anesthesia estimation and control," *IEEE Trans. Biomed. Eng.*, vol. 46, pp. 71–81, 1999.
[28] J. H. Lai and C. T. Lin, "Application of neural fuzzy network to pyrometer correction and temperature control in rapid thermal processing," *IEEE Trans. Fuzzy Syst.*, vol. 7, pp. 160–175, 1999.
[29] M. Vauhkonen, P. A. Karjalainen, and J. P. Kaipio, "A Kalman filter approach to track fast impedance changes in electrical impedance tomography," *IEEE Trans. Biomed. Eng.*, vol. 45, pp. 486–493, 1998.
[30] M. Arnold, W. H. R. Miltner, H. Witte, R. Bauer, and C. Braun, "Adaptive AR modeling of nonstationary time series by means of Kalman filtering," *IEEE Trans. Biomed. Eng.*, vol. 45, pp. 553–562, 1998.
[31] D. Sauter, B. J. Martin, N. Di Renzo, and C. Vomscheid, "Analysis of eye tracking movements using innovations generated by a Kalman filter," *Med. Biol. Eng. Comput.*, vol. 29, pp. 63–69, 1991.
[32] R. S. Parker, F. J. Doyle, III, and N. A. Peppas, "A model-based algorithm for glucose control in type I diabetic patients," *IEEE Trans. Biomed. Eng.*, vol. 46, pp. 148–157, 1999.
[33] R. Grieve, P. A. Parker, B. Hudgins, and K. Englehart, "Nonlinear adaptive filtering of stimulus artifact," *IEEE Trans. Biomed. Eng.*, vol. 47, pp. 389–395, 2000.
[34] B. Fetics, E. Nevo, C. H. Chen, and D. A. Kass, "Parametric model derivation of transfer function for noninvasive estimation of aortic pressure by radial tonometry," *IEEE Trans. Biomed. Eng.*, vol. 46, pp. 698–706, 1999.
[35] R. Johansson, *System Modeling and Identification*. Englewood Cliffs, NJ: Prentice-Hall, 1993.
[36] J. J. Wang, S. H. Liu, J. H. Hsieh, C. I. Chern, and C. Liu, "Fluctuation analysis of the continuous arterial blood pressue during Valsalva maneuver," *Biomed. Eng.: Appl., Basis and Commun.*, vol. 11, pp. 59–66, 1999.
[37] D. Brian, O. Anderson, and J. B. Moore, *Optimal Control: Linear Quadratic Method*. Englewood Cliffs, NJ: Prentice-Hall, 1989.
[38] D. G. Lainiotis, "A unifying framework for adaptive system I: Estimation," *Proc. IEEE*, vol. 64, pp. 1126–1143, 1976.
[39] C. T. Lin and C. S. G. Lee, *Neural Fuzzy Systems: A Neural-Fuzzy Synergism to Intelligent Systems*. Englewood Cliffs, NJ: Prentice-Hall, 1996.

Shing-Hong Liu received the B.S. degree in electronic engineering from the Feng-Chia University, Taichung, Taiwan, R.O.C., in 1990 and the M.S. degree in biomedical engineering from the National Cheng-Kung University, Tainan, Taiwan, in 1992. He is currently pursuing the Ph.D. degree in the Department of Electrical and Control Engineering at the National Chiao-Tung University, Hsinchu, Taiwan.

Since August 1994, he has been a Lecturer in the Department of Biomedical Engineering, Yuanpei Institute of Science and Technology, Hsinchu. His current research interests are digital signal processing, fuzzy control and biomedical instrument design.

Chin-Teng Lin (S'88–M'91–SM'98) received the B.S. degree in control engineering from the National Chiao-Tung University (NCTU), Hsinchu, Taiwan, R.O.C., in 1986 and the M.S.E.E. and Ph.D. degrees in electrical engineering from Purdue University, West Lafayette, IN, in 1989 and 1992, respectively.

Since August 1992, he has been with the College of Electrical Engineering and Computer Science, NCTU, where he is currently a Professor and Chairman of Electrical and Control Engineering Department. He served as the Deputy Dean of the Research and Development Office of NCTU from 1998 to 2000. His current research interests are fuzzy systems, neural networks, intelligent control, human–machine interface, image processing, pattern recognition, video and audio (speech) processing, and intelligent transportation system (ITS). He is the co-author of *Neural Fuzzy System—A Neuro-Fuzzy Synergism to Intelligent System* (Englewood Cliffs, NJ: Prentice-Hall), and the author of *Neural Fuzzy Control Systems with Structure and Parameter Learning* (Singapore: World Scientific).He has published over 60 journal papers in the areas of soft computing, neural networks, and fuzzy systems, including about 40 IEEE Transactions papers.

Dr. Lin is a member of Tau Beta Pi and Eta Kappa Nu. He is also a menber of the IEEE Computer Society, the IEEE Robotics and Automation Society, and the IEEE Systems, Man, and Cybernetics Society. He has been the Executive Council Member of Chinese Automation Association since 1998. He is the Chairman of IEEE Robotics and Automation Society Taipei Chapter since 2000, and an Associate Editor of IEEE TRANSACTIONS ON SYSTEMS, MAN, AND CYBERNETICS since 2001. He won the Outstanding Research Award granted by National Science Council (NSC), Taiwan, from 1997 to 2001, the Outstanding Electrical Engineering Professor Award granted by the Chinese Institute of Electrical Engineering (CIEE) in 1997, and the Outstanding Engineering Professor Award granted by the Chinese Institute of Engineering (CIE) in 2000. He was also elected to be one of the 38th Ten Outstanding Young Persons in Taiwan (2000).